Structural Characterization of the Transmembrane Domain from Subunit e of Yeast F_1F_o-ATP Synthase: A Helical GXXXG Motif Located Just under the Micelle Surface†

Huili Yao,‡ Rosemary A. Stuart,§ Sheng Cai,‡ and Daniel S. Sem*,‡

Chemical Proteomics Facility at Marquette, Department of Chemistry, Marquette University, P.O. Box 1881, Milwaukee, Wisconsin 53201-1881, and Department of Biological Sciences, Marquette University, Milwaukee, Wisconsin

Received August 2, 2007; Revised Manuscript Received December 10, 2007

ABSTRACT: F_1F_o-ATP synthase is a large multiprotein complex, including at least 10 subunits in the membrane-bound F_o-sector. One of these F_o proteins is subunit e (Su e), involved in the stable dimerization of F_1F_o-ATP synthase, and required for the establishment of normal cristae membrane architecture. As a step toward enabling structure−function studies of the F_o-sector, the Su e transmembrane region was structurally characterized in micelles. Based on a series of NMR and CD (circular dichroism) studies, a structural model of the Su e/micelle complex was constructed, indicating Su e is largely helical, and emerges from the micelle with Arg20 near the phosphate head groups. Su e only adopts this folded conformation in the context of the micelle, and is essentially disordered in DMSO, water or trifluoroethanol/water. Within the micelle the C-terminal Ala10−Arg20 stretch is helical, while the region N-terminal may be transiently helical, based on negative CSI (chemical shift index) values. The Ala10−Arg20 helix contains the $G^{14}XXXG^{18}$ motif, which has been proposed to play an important role in dimer formation with another protein from the F_o-sector. The Gly on the C-terminal end of this motif (Gly18) is slightly more mobile than the more buried Gly14, based on NMR order parameter measurements (Gly14 $S^2 = 0.950$; Gly18 $S^2 = 0.895$). Only one Su e transmembrane peptide is bound per micelle, and micelles are 22−23 Å in diameter, composed of 51 ± 4 dodecylphosphocholine detergent molecules. Although there is no evidence for Su e homodimerization via the transmembrane domain, potentially synergistic roles for N-terminal (membrane) and C-terminal (soluble) domain interactions may still occur. Furthermore, the presence of a buried charged residue (Arg7) suggests there may be interactions with other F_o-sector protein(s) that stabilize this charge, and possibly drive the folding of the N-terminal 9 residues of the transmembrane domain.

F_1F_o-ATP synthase catalyzes the synthesis of adenosine triphosphate (ATP)[1] from ADP, which is coupled to proton translocation across the mitochondrial inner membrane. Two distinct parts of this large multiprotein complex can be distinguished: the F_1-sector, which catalyzes ATP synthesis, and the membrane-bound F_o-sector, which mediates the proton transport (*1*). Crystal structures have been solved, first for bovine (*2*) and later for yeast (*3*) F_1-sectors at 2.8 Å and 2.9 Å, respectively. The F_o-sector, with the exception of the subunit c (Atp9)-oligomer (*4*−*6*) and secondary structure of subunit a (*7*), remains structurally uncharacterized. Subunit e (Su e) is one of at least 10 proteins associated with the membrane bound F_o-sector in *Saccharomyces cerevisiae* (*8*−*10*). Previous work has shown that Su e (and Su g) support the stable dimerization of the F_1F_o-ATP synthase complex (*8*, *9*, *11*, *12*), which leads to oligomerization in the inner mitochondrial membrane and the establishment of normal cristae membranes that penetrate into the mitochondrial matrix (*11*, *13*, *14*). Genetic knockout of either Su e or Su g leads to loss of normal cristae morphology in yeast, even though the F_1F_o-ATP synthase is still catalytically active (*9*, *11*, *14*, *15*). Both Su e and Su g are highly conserved across eukaryotes (*12*, *16*), and analysis of the Su e protein sequence indicates that it has a single hydrophobic N-terminal transmembrane region (∼20 residues) and a hydrophilic C-terminal region (∼75 residues) that resides in the intermembrane space. Su e is known to form homodimers as well as heterodimers with Su g, based on cross-linking studies (*12*,

† This research was supported by funding from Marquette University to D.S.S. and a U.S. Public Health Service Grant R01GM61573 to R.A.S. Studies made use of NMR instrumentation at the National Magnetic Resonance Facility at Madison (NIH: P41RR02301, P41GM66326) and the Chemical Proteomics Facility at Marquette (NIH-NSF instrumentation Grants S10 RR019012 and CHE-0521323). Remote connectivity was with Abilene/Internet2, funded by NSF (ANI-0333677).

* To whom correspondence should be addressed. E-mail: Daniel.sem@marquette.edu. Tel: 414-288-7859. Fax: 414-288-7066.

‡ Chemical Proteomics Facility at Marquette, Department of Chemistry.

§ Department of Biological Sciences.

[1] Abbreviations: ATP synthase, adenosine triphosphate synthase; CD, circular dichroism; CMC, critical micelle concentration; COSY, correlation spectroscopy; CPMG, Carr−Purcell−Meiboom−Gill; CSI, chemical shift index; CROX, chromium oxalate; DMSO, dimethyl sulfoxide; DOSY, diffusion ordered spectroscopy; DPC, dodecylphosphocholine; MALDI-TOF, matrix-assisted laser desorption ionization time of flight; NiEDDA, nickel ethylenediaminediacetic acid; NOESY, nuclear Overhauser effect spectroscopy; Su e, subunit e; TFE, trifluoroethanol.

10.1021/bi7015475 CCC: $40.75
Published on Web 01/26/2008

17, *46*). The C-terminal domain has been proposed to play a role in the dimerization of Su e, mediated by a predicted coiled-coil motif in this segment (*18*−*20*), while the N-terminal transmembrane domain contains a highly conserved GXXXG motif, which is commonly associated with protein−protein interactions in the transmembrane regions of dimerizing proteins (*18*−*20*). This GXXXG motif has been shown to play a role in the proper positioning of Su e within the F_o sector, possibly contributing to homo- and heterodimerization activites of Su e (*12*, *13*). As a step toward understanding these and other structure−function properties of Su e, we have structurally characterized the N-terminal transmembrane domain of yeast Su e, bound to dodecylphosphocholine (DPC) micelles.

In order to structurally characterize Su e, 2D NMR, CD (circular dichroism), DOSY (diffusion ordered spectroscopy), and paramagnetic probe methods were applied to the Su e transmembrane domain (resides 1−20) embedded in DPC micelles. Although this Su e domain adopts a random coil configuration in aqueous solution, bound to micelles it forms mainly α-helical structure, and emerges from the lipid surface with Arg20 near the phosphate head groups. No evidence of dimerization is observed, although it is possible there could be homodimerization through the GXXXG motif if the C-terminal domain were also present. The studies presented herein provide a foundation for future studies of full-length Su e, and of Su e in complex with other F_o-sector proteins.

MATERIALS AND METHODS

Peptide Synthesis. The N-terminal Su e transmembrane peptide (1−20, Ac-STVNVLRYSALGLGLFFGFR) was synthesized at the Protein and Nucleic Acid Shared Facility at the Medical College of Wisconsin (Milwaukee, WI). Note the amino acid residue numbering used here for Su e corresponds to that of the mature protein, as previous analysis had indicated that Su e undergoes N-terminal modification, with removal of the initial methionine residue and acetylation of Ser at position 2 (*9*). For this reason Ser is referred to here as position 1 of the peptide. The Su e peptide was obtained in 34 mg yield utilizing Fmoc chemistry, and was prepared using an Applied Biosystems 432A peptide synthesizer. N-Terminal acetylation was used to remove the charge, which would be absent on native yeast Su e, and the C-terminus was present as an amide. The MALDI-TOF mass spectrum showed a mass of 2259 *m*/*z* (expected = 2259 *m*/*z*), and HPLC indicated >95% purity. The peptide was aliquoted into single-use portions and stored at − 20 °C.

Another batch of peptide (~38 mg) was synthesized with three ^{15}N labeled glycine residues (G12, G14 and G18), which includes those present in the GXXXG motif. Glycine-^{15}N-Fmoc was purchased from Cambridge Isotope Laboratories and used for the synthesis. The HPLC and mass spectrum showed that the peptide was >95% pure, and had the expected molecular mass of 2262 m/z.

DPC Micelle Preparation. Fully deuterated DPC-d_{38} (dodecylphosphocholine-d_{38}) was purchased from Cambridge Isotope Laboratories. DPC has a critical micelle concentration (CMC) of ~1 mM (*21*), and the aggregation number of DPC micelles is reported to stabilize at ~56 molecules per micelle, with the micelle adopting a nearly spherical shape (*22*, *23*). Peptide:micelle samples were prepared by dissolving Su e peptide powder in a DPC micelle solution. The buffer was 20 mM potassium phosphate, pH 6.0, with 90% H_2O and 10% D_2O. The sample was placed in an eppendorf tube and sonicated in an ice water bath until the solution became clear. The solution was centrifuged after sonication, to give the final sample for the CD and NMR experiments. In order to achieve an approximate peptide:micelle ratio of 1:1, and a higher content of secondary structure, we finally chose the peptide:detergent molar ratio of 1:70 for NMR studies.

CD Spectroscopy. All CD experiments were performed at the Biochemistry department of the Medical College of Wisconsin. CD spectra were recorded for Su e (125 μM) in different concentrations of DPC micelles (20 mM potassium phosphate buffer, pH 6.0) in order to determine the best peptide:DPC ratio, which gives maximum secondary structure (i.e., folding). The CD measurements and the corresponding high tension voltage traces were made on a JASCO J710 spectropolarimeter with a 1 mm quartz cuvette at room temperature. Wavelengths were set from 190 to 250 nm. The response time (time constant), scan rate and bandwidth were 2 s, 50 nm/min, and 0.5 nm, respectively, and 8 scans were collected. Analysis of spectra was performed using the CD analysis software DICHROWEB (www.cryst.bbk.ac.uk/cdweb/html/home.html) (*24*).

NMR Spectroscopy. Samples of peptide in DPC micelles contained 2 mM peptide and 140 mM perdeuterated DPC. All NMR samples contained 20 mM phosphate buffer (pH 6.0) and 10% D_2O (or 5% D_2O). Perdeuterated DPC-d_{38} was used to reduce background signal from the detergent. A series of 2D NMR experiments were recorded on the Su e/DPC micelle solutions at 310 K, on 800 MHz or 600 MHz Varian spectrometers with cryoprobes. Water suppression was achieved with the WATERGATE pulse sequence (*25*).

The mixing times used for 2D ^{1}H−^{1}H NOESY experiments were 100, 150, 200, 300, and 400 ms. For 2D ^{1}H−^{1}H TOCSY experiments, spin-lock times were 40, 60, 80, and 100 ms. The spectral width was 10000 Hz in both dimensions at 800 MHz, and the spectra were collected with 3412 data points in the ω_2 and 512 data points in the ω_1 dimensions for both 2D ^{1}H−^{1}H NOESY and 2D ^{1}H−^{1}H TOCSY experiments. For the 2D DQF-COSY experiment, the spectral width was 6830.6 Hz in both dimensions at 600 MHz, and the spectrum was collected with 1746 data points in the ω_2 dimension and 256 data points in the ω_1 dimension. A 600 MHz 3D ^{15}N-edited NOESY experiment was run for the ^{15}N-glycine labeled Su e peptide; but parameters were set to acquire only the two ^{1}H dimensions, so the 2D showed only ^{1}H−^{1}H NOEs originating from ^{15}N attached protons. The spectral width for the ω_1 dimension was 5954 Hz and for ω_2 was 10000 Hz. The spectra were collected with 2048 data points in the direct dimension and 256 data points in the indirect dimension. Two such ^{15}N-filtered NOESY spectra were collected, with mixing times of 150 and 300 ms. Spectra were processed with NMRPipe (*44*) on an SGI Octane workstation, and assignments were completed using Sparky 3.110 (*26*). Chemical shifts were referenced to the HOD signal at the carrier frequency (4.64 ppm at 310 K).

Glycine Backbone Dynamics. In order to assess the dynamic properties of the glycine residues, ^{15}N relaxation rates (R_1 and R_2) and the ^{15}N-{^{1}H} heteronuclear NOE values were determined from NMR experiments on the Su e peptide containing three ^{15}N labeled glycines. The buffer conditions

were the same as described above. All NMR data were collected at 310 K on a 600 MHz Varian NMR spectrometer. For determining the ^{15}N spin−lattice (R_1) relaxation rates, 13 linear τ increments ranging from 0.05 to 1.2 s were used. For the ^{15}N spin−spin (R_2) relaxation rates, 15 linear τ increments between 4 ms and 200 ms were used with the CPMG (Carr−Purcell−Meiboom−Gill) pulse sequence (*45*). The pulse sequences used for ^{15}N R_1, R_2 and NOE measurements were gNT1, gNT2, and gNnoe in BioPack from Varian.

The ^{15}N R_1 and R_2 values were calculated by fitting the peak intensity (M) and the varied delay time (τ) to the following equation using SigmaPlot software:

$$M = M_0\, e^{-R\tau} \quad (1)$$

where R is R_1 or R_2 and M_0 corresponds to the equilibrium peak intensity.

For the ^{15}N-{^{1}H} NOE experiments, two 1D data sets were obtained with and without ^{1}H saturation. Saturation was achieved by irradiation at the middle of the amide proton frequency. ^{15}N-{^{1}H} NOE values were calculated as peak intensity ratios of the three ^{15}N labeled glycine signals obtained with and without ^{1}H saturation experiments. The relaxation and NOE data were processed using the Modelfree software package from Dr. Arthur Palmer (http://www.cumc.columbia.edu/dept/gsas/biochem/labs/palmer/software/modelfree.html). The basic input data for Modelfree includes R_1 values with errors, R_2 values with errors, ^{15}N NOE ratios with errors estimated from two sets of ^{15}N NOE experiments, and the correlation time τ_c, which can be calculated from T_1 and T_2 values using the following equations (*27*):

$$R_1 = (d^2/4)[3\tau_c/(1+\omega_S{}^2\tau_c{}^2) + \tau_c/(1+(\omega_I-\omega_S)^2\tau_c{}^2) + 6\tau_c/(1+(\omega_I+\omega_S)^2\tau_c{}^2)] + c^2[\tau_c/(1+\omega_S{}^2\tau_c{}^2)] \quad (2)$$

and

$$R_2 = (d^2/8)[4\tau_c + 3\tau_c/(1+\omega_S{}^2\tau_c{}^2) + \tau_c/(1+(\omega_I-\omega_S)^2\tau_c{}^2) + 6\tau_c/(1+(\omega_I+\omega_S)^2\tau_c{}^2) + 6\tau_c/(1+\omega_I{}^2\tau_c{}^2)] + (c^2/6)[4\tau_c + 3\tau_c/(1+\omega_S{}^2\tau_c{}^2)] \quad (3)$$

where $d = \mu_0 h\gamma_I\gamma_S/[(8\pi^2)r^3]$, $c^2 = \omega_S{}^2\Delta\sigma^2/3$, μ_0 is the permeability of free space, γ_I and γ_S are the gyromagnetic ratios of ^{1}H and ^{15}N, respectively, h is Planck's constant, r is the internuclear ^{1}H−^{15}N distance, ω_I and ω_S are the ^{1}H and ^{15}N Larmor frequencies, respectively, and $\Delta\sigma$ is the chemical shift anisotropy of the ^{15}N spin (assuming an axially symmetric chemical shift tensor). The symmetry axis of the chemical shift tensor is assumed to be collinear with the N−H bond vector. The calculated τ_c was 7.4 ns for 2 mM Su e peptide in 140 mM DPC.

Paramagnetic Measurements. Dipolar interactions with paramagnetic molecules enhance the relaxation rate of nuclei in their vicinity. The most obvious evidence for proximity to a paramagnetic probe is line broadening (a T_2 effect) or faster T_1 relaxation. In order to determine where the Su e peptide emerges from the micelle, the water-soluble paramagnetic reagent, CROX (chromium oxalate) and NiEDDA (nickel ethylenediaminediacetic acid) were added, and effects on T_1 relaxation measured for micelle-bound peptide. CROX and NiEDDA were chosen, based on their effective use in recent EPR studies of MsbA (the ATPase lipid A transporter found in the inner membranes of bacteria) for measuring how deeply that protein penetrated the membrane lipid (*28*), and earlier EPR characterization of membrane-embedded bacteriorhodopsin (*29*). Likewise, NMR-based paramagnetic probe studies have been used to characterize peptide/DPC micelles for over a decade (*30*, *31*), and one recent study presented the application of a variety of paramagnetic probes to characterize topology of the OmpX/DHPC mixed protein/micelle system (*32*).

The T_1 relaxation experiments were performed using the standard 1D inversion recovery presat pulse sequence in VnmrJ with satmode= "yyn". Spectral width was 7225 Hz, with 14450 data points, d_1 of 0.02 s, and 512 transients. For the T_1 relaxation study of 2 mM Su e in 140 mM DPC with no paramagnetic reagent present, d_2 was set as 0.001, 0.005, 0.01, 0.02, 0.05, 0.08, 0.1, 0.3, 0.5, 0.7, 0.8, 0.9, 1, 2, 4, and 8 s. For the T_1 relaxation study of 2 mM Su e in 140 mM DPC with 10 mM CROX or 50 mM NiEDDA present, d_2 was set as 0.001, 0.005, 0.01, 0.02, 0.04, 0.05, 0.06, 0.08, 0.1, 0.2, 0.4, 0.6, 0.8, 1, and 2 s. All data were processed using VnmrJ. It should be noted that although amides for residues throughout the Su e peptide sequence might be expected to provide a gradient of T_1 effects, correlated with depth of penetration into the micelle, the greatest effect was on the C-terminal Arg20 residue. Unfortunately, because of spectral overlap, it was not possible to determine T_1 values for other residues. Arg20, besides being most affected by paramagnetic probe, is also well-resolved from other residues, including Arg7. Furthermore, backbone and side chain NHs of Arg20 show correlated T_1 effects, also distinguishing it from Arg7.

Diffusion Ordered Spectroscopy (DOSY) Measurements. DOSY is an accurate method for determining the self-diffusion constant D of a molecular species in solution (*33*), which provides an estimate of its hydrodynamic radius. DOSY experiments were performed to determine if the Su e peptide is fully associated with the DPC micelles, and the approximate size and stoichiometry for the peptide:micelle complex. The DOSY spectra were acquired on a 750 MHz Bruker NMR spectrometer (at NMRFAM, UW−Madison) at 310 K. The observed signal intensity in the DOSY experiment is given by

$$I = I_0 \exp(-Dg^2\gamma^2\delta^2(\Delta - \delta/3 - \tau/2)) \quad (4)$$

where I_0 is the reference intensity, D is the diffusion coefficient, γ is the ^{1}H gyromagnetic ratio, δ is the total length of the defocusing/refocusing gradient pulses, Δ is the diffusion time (80 ms), and $\tau/2$ is the delay time between the two bipolar gradient pulses, which depends on spectrometer constraints, and g is the gradient strength, which was increased from 0 to 60 G cm^{-1}. From the determined D, the hydrodynamic radius r' of the peptide:DPC micelle could be calculated using the Stokes−Einstein equation:

$$D = kT/(6\pi\eta r') \quad (5)$$

where k is the Boltzmann constant, T is the absolute temperature, and η is the bulk viscosity of the solution, which is a function of solution conditions (e.g., temperature, salt,

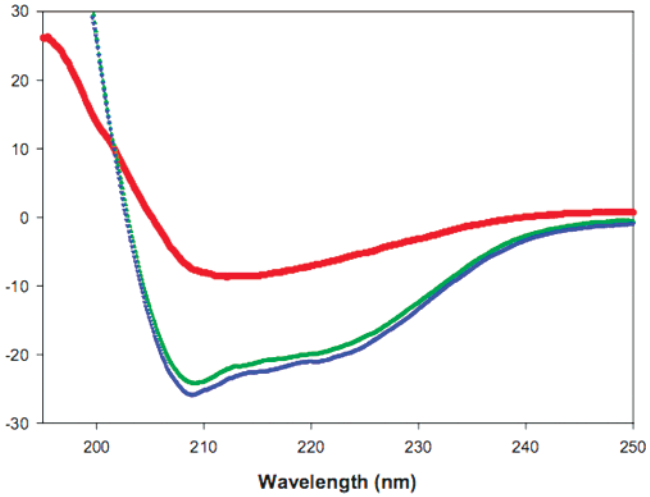

FIGURE 1: CD spectra of Su e peptide in DPC micelles. The peptide concentration was 125 μM in 20 mM potassium phosphate buffer, pH 6.0. The concentration ratios of peptide:DPC were 1:20 (red trace), 1:70 (green trace) and 1:86 (blue trace).

Table 1

Su e:DPC	α helix(%)	β sheet(%)	coil (%)	NRMSD[a]
1:20	13	39	48	0.555
1:70	45	22	34	0.096
1:86	51	24	25	0.096

[a] Normalized root-mean-square deviation.

and protein concentration). The η value was estimated from the diffusion constant of the residual HOD signal. From the calculated r', the molecular mass (MM) in daltons could be estimated by relating the equation of the volume of a sphere to the partial specific volume of a protein V_p. The V_p of an average protein is estimated to be 0.73×10^{-6} m^3 Da^{-1}. The protein/micelle assembly is also assumed to have a V_p of approximately 0.73×10^{-6} m^3 Da^{-1}.

$$r' = \{[(4)(0.73 \times 10^{-6})(\mathrm{MM})]/[(3\pi)(6.023 \times 10^{23})]\}^{1/3} \quad (6)$$

RESULTS AND DISCUSSION

Su e in DPC Micelles: Structural Characterization Using CD and DOSY. CD measurements of the Su e peptide were performed at different DPC:Su e ratios (Figure 1), and the secondary structure content of the Su e peptide was calculated from the spectra, as summarized in Table 1. At a low DPC:Su e ratio (20:1) there was no significant secondary structure for the Su e transmembrane peptide, which exhibited mainly random coil conformation with only ~13% α-helical content. However, α-helical content increases significantly when the DPC:Su e ratio increases to 70:1 or higher, indicating the lipid environment is required for folding. Likewise, NMR studies (especially 2D NOESY; not shown) indicate that the peptide folds better in DPC micelles than in water, d_6-DMSO or 30% trifluoroethanol (TFE). Within the DPC micelle, the Su e peptide appears to have ~50% α-helical content based on CD (note: calculations of α-helical content based on CD are only approximate, especially for peptides). But, additional studies were needed to establish whether all of the peptide is bound to the micelle, how many peptides are present per micelle, and how large the micelle complex is, relative to peptide (i.e., can the micelle accommodate the transmembrane domain). These questions could be addressed with DOSY experiments on the peptide:micelle complex.

From the DOSY spectrum of 2 mM Su e peptide in 140 mM DPC, it was observed that the peptide diffused at the same rate as the DPC micelles, with an average diffusion coefficient of 6.4×10^{-11} m^2 s^{-1}. That is, all of the Su e peptide appears to be embedded within the micelle. Based on this diffusion coefficient, a hydrodynamic radius of 22−23 Å was calculated. This is ~twice the length of a fully helical Su e peptide (*vide infra*), so the micelle can easily accommodate the transmembrane domain. Furthermore, the molecular mass of the peptide:DPC micelle could be estimated as 22.1 ± 1.4 kDa using eq 6. Based on the molecular weights of the Su e peptide (2259 g/mol) and the perdeuterated DPC (389 g/mol), this leads to an estimate of 51 ± 4 DPC detergent molecules that comprise one 22−23 Å micelle sphere, with one Su e peptide present per micelle. Previous molecular dynamics calculations suggest the shape of the DPC micelle is nearly spherical, being only slightly prolate (*22*). This micelle size is in close agreement with a published average aggregation number for DPC of 56 (*23*). The approximate 1:1 stoichiometry of peptide:micelle is based on the fact that micelles are present at 140 mM, so 140 mM/51 = 2.7 mM micelles, and the peptide is present at 2 mM and is fully bound to micelle. Although it is possible that some micelles contain >1 peptide, while others are vacant, NMR data discussed below show no evidence of interpeptide NOEs. In addition to DOSY data, titration of peptide with micelle supports the presence of monomeric peptide within a given micelle. That is, CD data indicate maximum helical content when there is a micelle:peptide stoichiometry of ~1:1, whereas if two peptides were bound per micelle, maximum helical content would be achieved at lower micelle concentrations. These DOSY and CD data, coupled with ^{15}N relaxation data that suggest a homogeneous structure, and the lack of interhelical NOEs, provide evidence that Su e is present within the micelle as a monomer rather than as a dimer. The DOSY and CD data together also suggest that the folding of Su e peptide is driven by the need to have at least one micelle present for each Su e peptide molecule; and peptide is much more soluble in micelle than in water, as expected. But the CD data do not distinguish between the possibilities of one long α-helix that oscillates between folded and unfolded states, versus a well-folded structure that is only partially helical. Furthermore, it is not known where the Su e peptide emerges from the micelle, and whether only one end of the peptide is close to the micelle surface (polar head groups), or whether it folds in such a way as to permit both ends to be near the surface. Although there is a C-terminal arginine (Arg20) that is likely to be near the micelle surface, there is another Arg (in position 7) that might also be expected to be near the polar surface of the micelle, if the peptide adopts a bent conformation, such as a helix−turn−helix. To answer these questions, a more detailed NMR structural analysis was pursued.

NMR-Based Structural Analysis. All spin systems for the Su e transmembrane peptide in DPC micelles were assigned based on chemical shifts and characteristic TOCSY and DQF-COSY cross-peak patterns. Sequence−specific assignments of backbone and most of the side chain resonances were made for the Su e transmembrane peptide bound to perdeuterated DPC micelles, using the sequential assignment

Table 2

residue	NH	αH	βH	others
S1	8.38	4.50	3.87, 3.95	
T2	8.47	4.21	4.06	γCH_3 1.20
V3	8.13	3.82	2.07	γCH_3 0.93, 0.99
N4	7.99	4.18	2.89, 2.92	γNH_2 6.75
V5	8.18	3.8	2.22	γCH_3 0.95, 1.05
L6	8.31	3.72		δCH_3 0.99, 0.91
R7	7.68	4.14	1.66, 1.82	γCH_2 1.53
				δCH_2 3.13
				NH 7.32
Y8	8.1	4.37	3.00, 3.09	2, 6 H 7.09
				3, 5 H 6.80
S9	8.32	4.47	3.84	
A10	8.37	4.22	1.19	
L11	7.94	4.14	1.88, 1.63	δCH_3 0.91
G12	8.33 ($^{15}N = 106.5$)	3.81, 3.73		
L13	8.2	4.20	1.48, 1.44	
G14	8.42 (^{15}N=106.4)	3.78		
L15	7.93	4.16	1.79, 1.45	δCH_3 0.86, 0.89
F16	8.03	4.59	3.19, 3.27	2, 6 H 7.30
				3, 5 H 7.28
				4 H 7.17
F17	7.98	4.46	3.29, 2.87	2, 6 H 7.43
				3, 5 H 7.31
				4 H 7.19
G18	7.8 ($^{15}N = 106.8$)	3.96, 3.87		
F19	8.14	4.61	3.19, 2.93	2, 6 H 7.31
				3, 5 H 7.27
R20	7.65	4.15	1.82, 1.64	γCH_2 1.52
				δCH_2 3.16
				NH 7.40, NH_2 6.76

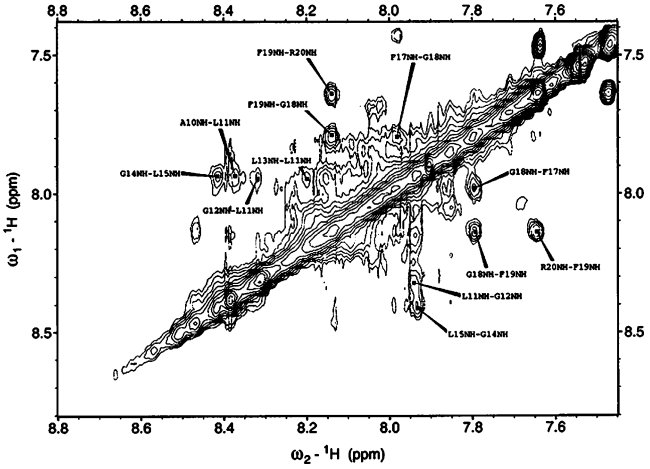

FIGURE 2: The d_{NN} region of the $^1H-^1H$ NOESY spectrum of 2 mM Su e transmembrane peptide in 140 mM DPC in 20 mM potassium phosphate buffer, pH 6.0 and 310 K.

strategy described by Wüthrich (*34*). Table 2 provides a summary of the assignments for the 20 residues of the micelle-bound Su e peptide. The d_{NN} region of the $^1H-^1H$ NOESY spectrum is shown in Figure 2, where it is evident that the strongest sequential connectivities are observed in the Ala10−Arg20 stretch of residues, consistent with this region being helical. The fingerprint ($d_{\alpha N}$) region was also assigned, but severe overlap left some assignment ambiguities that required specific labeling to resolve. The fingerprint region for a 2D ^{15}N-filtered $^1H-^1H$ NOESY of the labeled peptide (three ^{15}N-glycines) is shown in Figure 3, where a number of sequential and medium range connectivities are evident, including i to $i + 3$ NOEs associated with α-helical structure. A summary of $^1H-^1H$ NOE connectivities for the Su e peptide in DPC micelles is shown in Figure 4. The connectivities indicate an α-helical conformation for the Ala10−Arg20 stretch, with the typical pattern of d_{NN} (i, $i +$

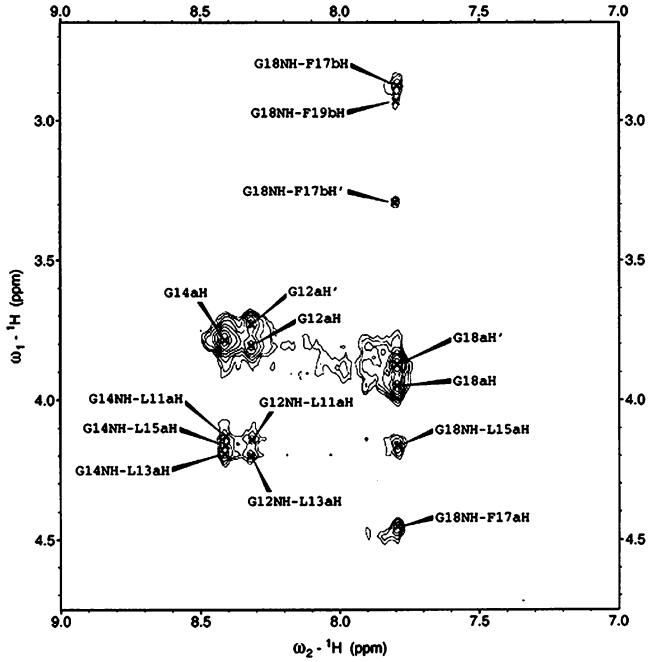

FIGURE 3: Fingerprint region of the $^{15}N-$filtered $^1H-^1H$ NOESY spectrum ($\tau_m = 150$ ms) of Su e peptide in DPC micelles (600 MHz with cryoprobe, and 310 K). Su e was 2 mM and DPC was 140 mM in potassium phosphate buffer, pH 6.0 with 10% D_2O.

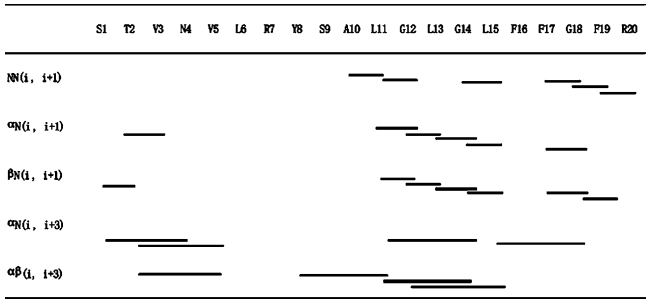

FIGURE 4: Summary of $^1H-^1H$ NOE connectivities for the Su e transmembrane peptide (Ser1−Arg20) bound to DPC micelles.

1), $d_{\alpha N}$ (i, $i + 3$), and $d_{\alpha\beta}$(i, $i + 3$) NOEs. The ^{15}N-filtered NOESY spectrum for the labeled peptide was very helpful in confirming many of the assignments. It not only permitted confirmation of resonance assignments for the three glycine residues, it aided with the sequential assignment of nearby residues, especially Leu11, Leu13, Leu15, Phe16, Phe17, and Phe19.

Since backbone H^α proton chemical shifts are sensitive to environment, confirmatory information on protein or peptide secondary structure can often be obtained by comparing the H^α chemical shifts to random-coil values, expressed as chemical shift index (CSI) values. Typically, H^α proton resonances for amino acids that are part of an α-helix tend to shift upfield (CSI < 0), whereas resonances for amino acids in β-sheet structures tend to shift downfield (CSI > 0), compared to random-coil chemical shifts (*35*, *36*). Most H^α proton resonances for micelle-bound Su e are shifted upfield (Figure 5), which is indicative of an α-helical structure. The fact that residues in the most N-terminal region (residues 2−9) are also shifted upfield may mean that they populate an α-helical state transiently.

In summary, these data clearly show that the region containing the GXXXG motif is α-helical, although there

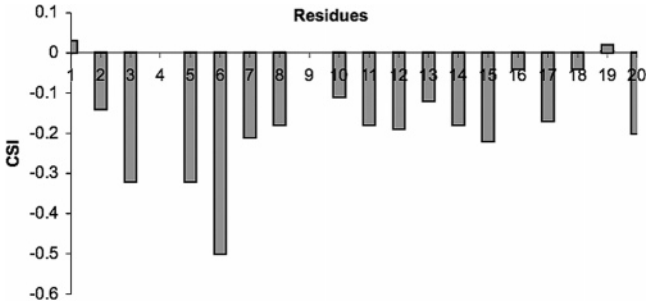

FIGURE 5: H^{α} CSI plot for the Su e transmembrane peptide (Ser1−Arg20) bound to DPC micelles.

may be some break in helicity at the center of the GXXXG motif. But this is difficult to conclude with certainty, as the lack of medium range connectivities in this region could also be attributed to the highly overlapped nature of the fingerprint region. Longer range NOEs were observed from Ser1 to Val5 and from Tyr8 to Gly18, possibly from transiently populated state(s), but there were not enough long range NOEs to permit a structure calculation. What is clear though, is that the region from Ala10-Arg20 is α-helical. This is the region containing the GXXXG dimerization motif, so the motif is clearly helical even in the absence of dimerization with another Su e molecule or with Su g or with other F_o-sector proteins. The region N-terminal to Ala10 might not be well-folded, but may become folded in the context of interactions with other F_o-sector proteins.

Backbone Dynamics for GXXXG Motif Glycines. Given the potentially important role of the GXXXG motif in Su e and other membrane embedded proteins, and the possibility of a helical break in the middle of this motif, we wondered if these residues were part of a flexible/mobile region that rigidifies only when the dimerization partner is encountered, or in the context of the intact F_o-sector. To partially address this question, backbone motion on the picosecond to nanosecond time scale was assessed using dynamics measurements of the ^{15}N-labeled glycine residues. Peptide backbone dynamics and flexibility were quantified using the Lipari−Szabo formalism (*37*, *38*). The generalized order parameters, S^2, were calculated from the experimentally measured R_1, R_2, and heteronuclear NOE values for the three ^{15}N-labeled glycine residues (N−H vectors). When measuring the ^{15}N R_1 and R_2 values, it was clear that peak intensities were very well defined by a single-exponential function, indicating that the motional freedom of the peptide was identical for all Su e molecules. That is, the Su e structure is homogeneous, and is therefore not a mixture of monomeric/dimeric states with different motional regimes for the GXXXG motif. The measured R_2 values are 11.2 ± 0.4 s^{-1}, 11.3 ± 0.4 s^{-1}, and 10.4 ± 0.4 s^{-1} for G14, G12 and G18 respectively; the measured R_1 values are 1.80 ± 0.034 s^{-1}, 1.74 ± 0.029 s^{-1}, and 1.78 ± 0.035 s^{-1} for G14, G12 and G18 respectively; and, the measured ^{15}N NOEs are 0.74 ± 0.02, 0.74 ± 0.01, and 0.59 ± 0.02 for G14, G12 and G18 respectively. Relatively high NOE values (>0.6) are indicative of residues that are located in regions with restricted internal motions.

The calculated S^2 values are 0.988, 0.950, and 0.895 for G12, G14 and G18, respectively. Values of S^2 between 0.85 and 1 are typical of a well-defined and somewhat rigid structure. All three glycine residues have similar motional characteristics, with order parameters between 0.89 and 0.99. Such high values for S^2 are consistent with reasonably well-defined secondary structure, and have been observed previously for peptides embedded in micelles (*39*, *40*). Of the three labeled glycines, G18 has a slightly lower S^2, which indicates it has more motional freedom. This motional freedom is probably due to G18's location near the C-terminus of the Su e transmembrane helix. But there is not significant motion for any of these glycine residues, consistent with the GXXXG motif having a fairly well-defined structure, even in the absence of binding partners and outside of the context of the intact F_o-sector. Future studies will be directed to dynamics measurements of other selectively labeled Su e residues, and in the context of other F_0 sector proteins.

A Su e:DPC Micelle Structural Model. The Su e transmembrane peptide is clearly α-helical for residues Ala10−Arg20, which includes the GXXXG dimerization motif. The region N-terminal to this may also populate an α-helical structure. But lack of more medium range connectivities leads us to propose that residues Thr2−Ser9, and possibly residues Phe16−Arg20, may be only transiently helical, and the overall helical content may be lower than predicted from CD data. In contrast though, high S^2 values argue that the Phe16−Arg20 stretch may be somewhat more ordered (or else that the helical/unstructured transition is a slow exchange process within the micelle). This helical structure is only adopted within the micelle, and not in water, TFE/water or DMSO. This requirement for a proper membrane-like environment is commonly required for proper folding of transmembrane proteins and peptides (*41*, *42*). DOSY results indicate that the Su e peptide/micelle complex has a hydrodynamic radius of 22−23 Å, corresponding to ∼50 DPC lipid molecules per Su e peptide. Indeed, helical structure is only present at DPC:peptide ratios that are at least this high. NMR protein dynamics studies of the Su e glycines (G12, G14, and G18), which span the conserved GXXXG motif, suggest this helix is highly structured and rigid, although the C-terminal Gly ($G^{14}XXX\boldsymbol{G}^{18}$) is slightly more mobile. This residue is near the C-terminal end of the Ala10−Arg20 helix, where the transmembrane region may begin to emerge from the micelle. Certainly, emergence from the micelle must occur at some point in this vicinity, since the C-terminal domain, which occurs soon after this transmembrane domain, is known to reside in the intermembrane space (*8*). Where the transmembrane peptide emerges from the micelle, and how it is oriented (approximately) within the micelle, was next explored using water-soluble paramagnetic agents.

Addition of water-soluble paramagnetic agents confirms that the C-terminal region is more solvent exposed than the rest of the peptide, and represents the point at which Su e would enter the intermembrane space. The paramagnetic T_1 relaxation study (Figure 6) indicates that one residue in the Su e peptide experiences a faster relaxation rate compared to other residues, due to presence of the paramagnetic reagent CROX or NiEDDA, which resides predominantly in the aqueous layer. The proton signal that relaxes fastest in Figure 6 is at ∼6.78 ppm, which is for Arg20. In this inversion−recovery experiment, at $\tau = 0.04$ s a positive signal appeared for that resonance, but all other protons started to appear

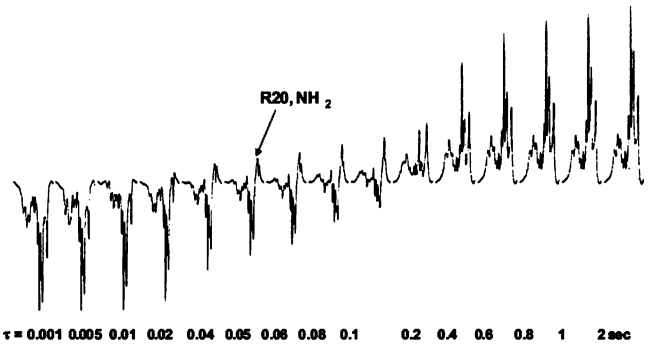

FIGURE 6: T_1 relaxation study of Su e peptide embedded in DPC micelles (concentrations as in Figure 2), in the presence of 10 mM CROX at 310 K and 600 MHz. The array of d_2 values used in the inversion recovery pulse sequence is shown at the bottom of the spectra.

positive only at around $\tau = 0.1$ s. Therefore, this Arg20 proton experiences a slightly stronger paramagnetic effect, due to exposure to solvent on the outside of the micelle.

To summarize, we propose a Su e:DPC model with the N-terminus of the transmembrane domain buried deeply in the micelle, and emerging from the micelle with the C-terminal Arg20 interacting with the negatively charged polar head groups while Phe19 is still buried in the hydrophobic lipid layer. Because CSI values for the entire peptide are only slightly negative (Figure 5), it could be that peptide adopts a somewhat loose helical state. This would be consistent with the sparsity of medium range connectivities (Figure 4), even in the Ala10−Arg20 stretch. While the first 9 residues of Su e do not show NOE connectivities consistent with helix, the presence of negative CSI values do suggest helix. As such, we suspect that this region may at least transiently populate a helical state, which may adjust to a properly folded conformation in the intact F_o-sector. Indeed, it would be unusual to have an unstructured region with unsatisfied H-bond donor/acceptors buried within a low-dielectric medium, so we suspect this transient unfolded state is an artifact of our system, which lacks the other F_o-sector proteins that may be needed to fully stabilize the N-terminal secondary structure. Furthermore, we conclude also from our data that Arg7 appears to be buried in the micelle, indicating that it would be located within the lipid bilayer of the mitochondrial inner membrane, an unusual position for a potentially charged residue. We suspect therefore that Arg7 will participate in interactions with other F_o-sector proteins, which may have complementary negative charges. This would be consistent with the highly conserved nature of the R^7YSAL motif in which Arg7 is located. One potential interaction partner is Su g. Although Su g is known to dimerize with Su e through their respective transmembrane segments and in a manner which is not dependent on the integrity of their respective conserved GXXXG motifs (*15*, *17*, *46*), it is unlikely that Su g provides charge stabilization for Arg7. Although many Su g proteins contain a negatively charged residue (Glu) within their GXXXG motif (*17*), it would not be properly positioned to interact with Arg7. Because the Su e and Su g GXXXG motifs immediately precede the positively charged residues (Arg20 in Su e and Arg106 in Su g) thought to interact with the phospholipid phosphates, they are buried at approximately the same depth in the bilayer, which means that the properly positioned amino acid on Su g for interaction with Arg7 of Su e would be located 7−8 residues to the N-terminus of the Su g GXXXG motif (i.e., not in the GXXXG motif). One could then ask if there is a potential interacting residue in Su g, at the appropriate position N-terminal to GXXXG. But *Saccharomyces cerevisiae* Su g does not contain any negatively charged amino acid in the region 7−8 residues N-terminal to the GXXXG motif; although Su g peptides from other organisms do contain a Glu in this position. Still, if Su e/Su g GXXXG motifs were to pack in the typical manner, with the two peptides crossing each other at ∼40° angles (*43*), this would position Arg7 of Su e far from the corresponding region of Su g (Gln or Glu 93). A more likely interaction between Su e and Su g might be similar to that proposed by Bustos and Velours (*46*), where the phenylalanines of Su e (Phe16/Phe17 in our numbering) interact with Tyr98 of Su g; and the Glu93 of Su g has no interaction with Su e. We therefore suspect that another inner membrane protein (not Su g), most likely another F_o-sector protein, may interact with and stabilize the buried Arg7 of Su e.

Finally, our data do not support a model of Su e homodimerization via their transmembrane domains, as there was no evidence of Su e/Su e homodimerization within the micelle. This observation is consistent with previous results (*12*, *15*, *17*) where mutation of the highly conserved GXXXG motif of Su e did not affect Su e/Su e dimerization, as judged by chemical cross-linking experiments. Thus, we consider it more likely that protein−protein interactions occurring via the conserved coiled-coil motifs in the soluble intermembrane space domain, i.e., C-terminal of Arg20, are responsible for any Su e−Su e homodimerization.

ACKNOWLEDGMENT

We thank Dr. Gabriel Cornilescu (UW−Madison) for assistance with DOSY measurements, Dr. Candice Klug (Medical College of Wisconsin) for CROX, NiEDDA and for recommending the paramagnetic probe studies, and Dr. Francoise A. Van den Bergh (Medical College of Wisconsin) for assistance with CD measurements.

REFERENCES

1. Capaldi, R. A., and Aggeler, R. (2002) Mechanism of the F(1)F-(0)-Type ATP Synthase, a Biological Rotary Motor, *Trends Biochem. Sci. 27*, 154−160.
2. Abrahams, J. P., Leslie, A. G., Lutter, R., and Walker, J. E. (1994) Structure at 2.8 Å Resolution of F_1F_o-ATPase from Bovine Heart Mitochondria, *Nature 370*, 621−628.
3. Stock, D., Leslie, A. G., and Walker, J. E. (1999) Molecular Architecture of the Rotary Motor in ATP Synthase, *Science 286*, 1700−1705.
4. Rastogi, V. K., and Girvin, M. E. (1999) NMR Studies of Subunit c of the ATP Synthase F_o-Sector, *Nature 402*, 263−268.
5. Girvin, M. E., and Fillingame, R. H. (1995) Determination of Local Protein Structure by Spin Label Difference 2D NMR: The Region Neighboring Asp61 of Subunit c of F_1F_o ATP Synthase, *Biochemistry 34*, 1635−1645.
6. Stock, D., Leslie, A. G., Walker, J. E. (1999) Molecular Architecture of the Rotary Motor in ATP Synthase, *Science 286* 1700−1705.
7. Dmitriev, O. Y., Abildgaard, F., Markley, J. L., and Fillingame, R. H. (2004) Backbone ^{1}H, ^{15}N and ^{13}C Assignments for the Subunit a of the *E. coli* ATP Synthase, *J. Biomol. NMR 29*, 439−440.
8. Arnold, I., Bauer, M. F., Brunner, M., Neupert, W., and Stuart, R. A. (1997) Yeast Mitochondrial F_1F_o-ATPase: The Novel Subunit e is Identical to Tim11, *FEBS Lett. 411*, 195−200.

9. Arnold, I., Pfeiffer, K., Neupert, W., Stuart, R. A., and Schagger, H. (1998) Yeast Mitochondrial F_1F_o-ATP Synthase Exists as a Dimer: Identification of Three Dimer-Specific Subunits, *EMBO J. 17*, 7170−7178.
10. Velours, J., and Arselin, G. (2000) The Saccharomyces Cerevisiae ATP Synthase, *J. Bioenerg. Biomembr. 32*, 383−390.
11. Paumard, P., Vaillier, J., Coulary, B., Schaeffer, J., Soubannier, V., Mueller, D. M., Brethes, D., di Rago, J. P., and Velours, J. (2002) The ATP Synthase is Involved in Generating Mitochondrial Cristae Morphology, *EMBO J. 21*, 221−230.
12. Brunner, S., Everard-Gigot, V., and Stuart, R. A. (2002) Su e of the Yeast F_1F_o-ATP Synthase Forms Homodimers, *J. Biol. Chem. 277*, 48484−48489.
13. Arselin, G., Giraud, M. F., Dautant, A., Vaillier, J., Brethes, D., Coulary-Salin, B., Schaeffer, J., and Velours, J. (2003) The GxxxG Motif of the Transmembrane Domain of Subunit e is Involved in the dimerization/oligomerization of the Yeast ATP Synthase Complex in the Mitochondrial Membrane, *Eur. J. Biochem. 270*, 1875−1884.
14. Arselin, G., Vaillier, J., Salin, B., Schaeffer, J., Giraud, M. F., Dautant, A., Brethes, D., and Velours, J. (2004) The Modulation in Subunits e and g Amounts of Yeast ATP Synthase Modifies Mitochondrial Cristae Morphology, *J. Biol. Chem. 279*, 40392−40399.
15. Everard-Gigot, V., Dunn, C. D., Dolan, B. M., Brunner, S., Jensen, R. E., and Stuart, R. A. (2005) Functional Analysis of Subunit e of the F_1F_o-ATP Synthase of the Yeast Saccharomyces Cerevisiae: Importance of the N-Terminal Membrane Anchor Region, *Eukaryotic Cell 4*, 346−355.
16. Schagger, H., and Pfeiffer, K. (2000) Supercomplexes in the Respiratory Chains of Yeast and Mammalian Mitochondria, *EMBO J. 19*, 1777−1783.
17. Saddar, S., and Stuart, R. A. (2005) The Yeast F(1)F(0)-ATP Synthase: Analysis of the Molecular Organization of Subunit g and the Importance of a Conserved GXXXG Motif, *J. Biol. Chem. 280*, 24435−24442.
18. Kleiger, G., Grothe, R., Mallick, P., and Eisenberg, D. (2002) GXXXG and AXXXA: Common Alpha-Helical Interaction Motifs in Proteins, Particularly in Extremophiles, *Biochemistry 41*, 5990−5997.
19. Senes, A., Ubarretxena-Belandia, I., and Engelman, D. M. (2001) The Calpha---H...O Hydrogen Bond: A Determinant of Stability and Specificity in Transmembrane Helix Interactions, *Proc. Natl. Acad. Sci. U.S.A. 98*, 9056−9061.
20. Russ, W. P., and Engelman, D. M. (2000) The GxxxG Motif: A Framework for Transmembrane Helix-Helix Association, *J. Mol. Biol. 296*, 911−919.
21. Lauterwein, J., Bosch, C., Brown, L. R., and Wuthrich, K. (1979) Physicochemical Studies of the Protein-Lipid Interactions in Melittin-Containing Micelles, *Biochim. Biophys. Acta 556*, 244−264.
22. Wymore, T., Gao, X. F., and Wong, T. C. (1999) Molecular Dynamics Simulation of the Structure and Dynamics of a Dodecylphosphocholine Micelle in Aqueous Solution, *J. Mol. Struct. 485-486*, 195−210.
23. Lazaridis, T., Mallik, B., and Chen, Y. (2005) Implicit Solvent Simulations of DPC Micelle Formation, *J. Phys. Chem. B 109*, 15098−15106.
24. Whitmore, L., and Wallace, B. A. (2004) DICHROWEB, an Online Server for Protein Secondary Structure Analyses from Circular Dichroism Spectroscopic Data, *Nucleic Acids Res. 32*, W668−W673.
25. Piotto, M., Saudek, V., and Sklenar, V. (1992) Gradient-Tailored Excitation for Single-Quantum NMR Spectroscopy of Aqueous Solutions, *J. Biomol. NMR 2*, 661−665.
26. Goddard, T. D., and Kneller, D. G. *Sparky*, UCSF, California.
27. Kay, L. E., Torchia, D. A., and Bax, A. (1989) Backbone Dynamics of Proteins as Studied by ^{15}N Inverse Detected Heteronuclear NMR Spectroscopy: Application to Staphylococcal Nuclease, *Biochemistry 28*, 8972−8979.
28. Buchaklian, A. H., Funk, A. L., and Klug, C. S. (2004) Resting State Conformation of the MsbA Homodimer as Studied by Site-Directed Spin Labeling, *Biochemistry 43*, 8600−8606.
29. Altenbach, C., Greenhalgh, D. A., Khorana, H. G., and Hubbell, W. L. (1994) A Collision Gradient Method to Determine the Immersion Depth of Nitroxides in Lipid Bilayers: Application to Spin-Labeled Mutants of Bacteriorhodopsin, *Proc. Natl. Acad. Sci U.S.A. 91*, 1667−1671.
30. Lauterwein, J., Bosch, C., Brown, L. R., and Wuthrich, K. (1979) Physiochemical Studies of the Protein-Lipid Interactions in Melittin-Containing Micelles, *Biochim. Biophys. Acta 556*, 244−264.
31. Brown, L. R., Bosch, C., and Wuthrich, K. (1981) Location and Orientation Relative to the Micelle Surface for Glucagon in Mixed Micelles with Dodecylphosphocholine, *Biochim. Biophys. Acta 642*, 296−312.
32. Hilty, C., Wider, G., Fernandez, C., and Wuthrich, K. (2004) Membrane Protein-Lipid Interactions in Mixed Micelles Studied by NMR Spectroscopy with the use of Paramagnetic Reagents, *ChemBioChem 5*, 467−473.
33. Johnson, C. S., Jr. (1999) Diffusion Oriented Nuclear Magnetic Resonance Spectroscopy: Principles and Applications, *Prog. Nucl. Magn. Reson. Spectrosc. 34*, 203−256.
34. Wuthrich, K. (1986) *NMR of Proteins and Nucleic Acids*, John Wiley & Sons, New York.
35. Wishart, D. S., Sykes, B. D., and Richards, F. M. (1992) The Chemical Shift Index: A Fast and Simple Method for the Assignment of Protein Secondary Structure through NMR Spectroscopy, *Biochemistry 31*, 1647−1651.
36. Wishart, D. S., and Sykes, B. D. (1994) Chemical Shifts as a Tool for Structure Determination, *Methods Enzymol. 239*, 363−392.
37. Lipari, G., and Szabo, A. (1982) Model-Free Approach to the Interpretation of Nuclear Magnetic Relaxation in Macromolecules. 1. Theory and Range of Validity, *J. Am. Chem. Soc. 104*, 4546−4559.
38. Lipari, G., and Szabo, A. (1982) Model-Free Approach to the Interpretation of Nuclear Magnetic Resonance Relaxation in Macromolecules. 2. Analysis of Experimental Results, *J. Am. Chem. Soc. 104*, 4559−4570.
39. Jarvet, J., Zdunek, J., Damberg, P., and Graslund, A. (1997) Three-Dimensional Structure and Position of Porcine Motilin in Sodium Dodecyl Sulfate Micelles Determined by ^{1}H NMR, *Biochemistry 36*, 8153−8163.
40. Lerch, M., Gafner, V., Bader, R., Christen, B., Folkers, G., and Zerbe, O. (2002) Bovine Pancreatic Polypeptide (bPP) Undergoes Significant Changes ib Conformation and Dynamics upon Binding to DPC Micelles, *J. Mol. Biol. 322*, 1117−1133.
41. Vinogradova, O., Sonnichsen, F., and Sanders, C. R.,2nd. (1998) On Choosing a Detergent for Solution NMR Studies of Membrane Proteins, *J. Biomol. NMR 11*, 381−386.
42. Sanders, C. R., and Oxenoid, K. (2000) Customizing Model Membranes and Samples for NMR Spectroscopic Studies of Complex Membrane Proteins, *Biochim. Biophys. Acta 1508*, 129−145.
43. Walters, R. F., and DeGrado, W. F. (2006) Helix-Packing Motifs in Membrane Proteins, *Proc. Natl. Acad. Sci. U.S.A. 103*, 13658−13663.
44. Delaglio, F., Grzesiek, S., Vuister, G. W., Zhu, G., Pfeifer. J., and Bax, A. (1995) NMRPipe: a multidimensional spectral processing system based on UNIX pipes, *J. Biomol. NMR 6*, 277−293.
45. Loria, J. P., Rance, M., and Palmer, A. G., III (1999) A relaxation-compensated Carr-Purcell-Meiboom-Gill sequence for characterizing chemical exchange by NMR spectroscopy, *J. Am. Chem. Soc. 121*, 2331−2332.
46. Bustos, D. M., and Velours, J. (2005) The modification of the conserved GXXXG motif of the membrane spanning segment of subunit g destabilizes the supramolecular species of yeast ATP synthase, *J. Biol. Chem. 280*, 29004−29010.

BI7015475